Hindawi Publishing Corporation
ISRN Tribology
Volume 2013, Article ID 254705, 6 pages
http://dx.doi.org/10.5402/2013/254705

Research Article

Contribution to the Modelling of the Tribological Surface Transformations

G. Antoni[1,2]

[1] *Laboratoire de Mécanique et d'Acoustique, UPR CNRS 7051, 31 Chemin Joseph-Aiguier, 13402 Marseille Cedex 20, France*
[2] *Université de Provence, 3 Place Victor Hugo, 13331 Marseille Cedex 03, France*

Correspondence should be addressed to G. Antoni; antoni@lma.cnrs-mrs.fr

Received 24 April 2012; Accepted 23 May 2012

Academic Editors: F. Nair, Z. Wen, and H. Xing

When solids are subjected to tribological loads, structural changes can occur both at the surface and in depth, immediately below the loaded area; in the case of some materials, especially metals, these changes are known as solid-solid phase transformations or Tribological Surface Transformations (TSTs). A thermomechanical model is presented in the present study in order to describe these TSTs. The ability of the model to take account TSTs is assessed with a 2D finite element analysis.

1. Introduction

Tribological Surface Transformations (TSTs) which occur in various types of contacts (such as fretting, wheel/rail contact, and impact), are generally structural changes undergone by the metallic materials involved, including some metal alloys (steel, cast iron, maraging, titanium alloys, and aluminum alloys), as the result of solid-solid phase transformations. These transformations, which are also known as "White Etching Layers" (WELs), are characterized by the development of a white phase on the treads of the rails, which is visible under electron microscopy, at depths ranging from several nanometers to more than 100 μm, depending on the material in question. It has been attempted in many studies to determine what causes TSTs origin, see Colombié [1], Blanchard [2], and Sauger [3] for the fretting and Sekkal [4] for the impact. Most previous studies on WELs have focused on the case of wheel/rail contacts (cf. Figure 1) (see, e.g., [5–8]). The results obtained show that the micro-hardness of TSTs generally ranges from 700 to 1000 H_v in the case of materials such as aluminum alloys and steels, while the initial hardness of the rails is about 300 H_v. The chemical composition of TSTs is identical to that of the original material, that is, only the metallurgical structure of the rails undergoes a change. In the case of rail problems, some authors have attributed the development of TSTs to the combined normal and shear stresses present in wheel/rail contacts [8, 9]. On the other hand, Archard and Rowntree [10], Ahlström and Karlsson [11] have attributed this process to the presence of high temperatures known as "Flash Temperatures" of around 1000°C in the wheel/rail contact area during a very short period of only a few seconds. Baumann et al. [12] suggested that the high normal and shear stresses combined with a significant temperature increase (of around 150 to 200°C) in the contact zone may cause the formation of TSTs near the surface, where the mechanical loads are applied; this assumption was supported by Lojkowski et al. [6], Jirásková et al. [13].

Generally, during phase transformations under mechanical loads, an anomalous plastic flow is superimposed with the classical plasticity, existing in the metallic materials, for stresses levels which are much lower than the initial strength of the softest phase. The so-called "Transformation Induced Plasticity" (TRIP) process has been explained by Greenwood and Johnson [14] who suggested that the plasticity responsible for these transformations may be due to the orientation of the plastic flow by the external stress around the new phase. In other words, the microplasticity generated by the incompatibility between the volumes involved in the phase transformation may be oriented by the external stress applied. Many models have been presented to account for TRIP phenomena, such as that developed by Leblond et al. [15], Leblond [16], Videau et al. [17, 18], Fischer et al. [19], Taleb and Sidoroff [20], and Taleb and Petit [21].

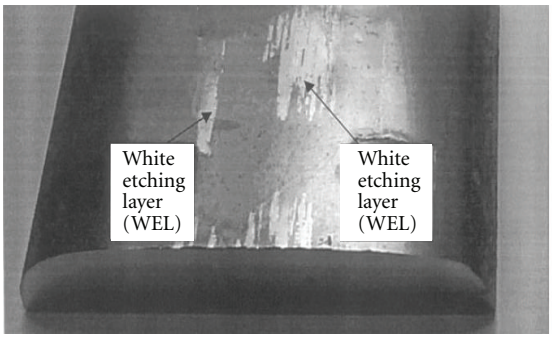

(a)

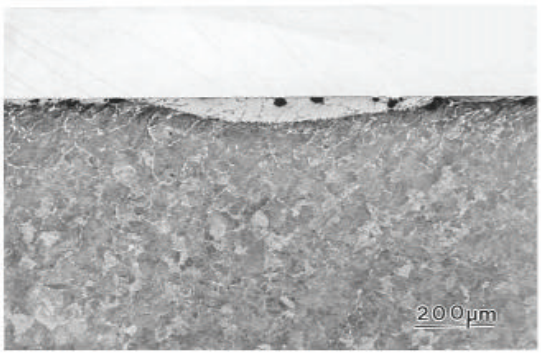

(b)

Figure 1: (extract from [5]) (a) macroscopic view on the tread of a rail (S54/900A steel) showing TSTs or "White Etching Layer." (b) Transverse cross-section of the upper part of a rail (a). The parent phase (grey part) is pearlite, which still remains in the rail when TSTs have developed and the daughter phase (white part), occurring at the surface, is "quasi-martensite."

In agreement with Baumann et al. [12], the main assumption adopted in the present study is that the thermomechanical coupling process lead to the TSTs formation since the mechanical loads and the temperature increase—due to the friction occurring in the wheel/rail contact area—can be highly correlated. Taking into account the above assumption and the previous works on TRIP processes, a thermomechanical model [22, 23], is proposed to describe the TSTs initiation and development near the surface where the mechanical loads are applied.

2. A Thermomechanical Model to Irreversible Solid-Solid Phase Transformations and TSTs

Considering a continuum thermoelasto-viscoplastic solid occupying a spatial region $\Omega \in \mathbb{R}^3$, and restricted to the small strains, the total strain ϵ consists in an elastic classical (visco)plasticity and TRIP-like strain components, the additive decomposition of total strain may be written as follows:

$$\epsilon = \epsilon^{te} + \epsilon^{pc} + \epsilon^{pz}, \tag{1}$$

where ϵ^{te}, ϵ^{pc}, and ϵ^{pz} represent the thermoelastic, classical (visco)plasticity, and TRIP-like parts of the total strain, respectively.

Afterwards, each above strain tensor (1) is decomposed, respectively, into its spherical and deviatoric parts as,

$$\begin{gathered}\epsilon = \frac{1}{3}\operatorname{Tr}(\epsilon)\,G + e; \qquad \epsilon^{te} = \frac{1}{3}\operatorname{Tr}\left(\epsilon^{te}\right)G + e^{e};\\ \epsilon^{pc} = e^{pc}; \qquad \epsilon^{pz} = \frac{1}{3}\,f(z)\,G + e^{pz}\\ \text{with } \operatorname{Tr}\left(\epsilon^{te}\right) = \operatorname{Tr}\left(\epsilon^{e}\right) + 3\alpha\left(T - T_i\right), \qquad f(z) = \frac{z}{\kappa},\end{gathered} \tag{2}$$

where G denotes the metric tensor, ϵ^e (respectively e^e) is elastic strain tensor (respectively deviatoric tensor), T is the absolute temperature, T_i is initial temperature, $\alpha > 0$ is the thermal expansion coefficient, the classical (visco)plasticity strain tensor, ϵ^{pc}, has only a deviatoric part (isochoric plasticity in metallic materials case), $f(z)$ denotes a density variation involving the TRIP-like process, $z \in [0,1]$ is the mass fraction of the daughter phase (where the partial density of the daughter phase, ρ^d, is given by $\rho^d = z\rho$), and $\kappa > 0$ is a material parameter characterizing the density variation during phase transformation.

Initially, the material in question is nontransformed (i.e., $z_i = 0$, $f(z_i) = 0$, and $e_i^{pz} = 0$) at the temperature T_i, the Helmholtz free energy potential per unit mass is written (with v an isotropic hardening variable associated with classical plasticity):

$$\begin{aligned}&\psi\left(T, \operatorname{Tr}(\epsilon), e, e^{pc}, e^{pz}, z, v\right)\\ &\quad = -C_\epsilon\frac{\left(T - T_i\right)^2}{2T_i} + \frac{1}{2\rho_i}hv^2\\ &\qquad + \frac{1}{2\rho_i}\frac{3\lambda + 2\mu}{3}\left[\operatorname{Tr}(\epsilon) + f(z)\right]^2\\ &\qquad + \frac{\mu}{\rho_i}\left[\left(e - e^{pc} - e^{pz}\right) : \left(e - e^{pc} - e^{pz}\right)\right]\\ &\qquad - \frac{1}{\rho_i}\left(3\lambda + 2\mu\right)\alpha\left(T - T_i\right)\left[\operatorname{Tr}(\epsilon) + f(z)\right]\\ &\qquad + \frac{\delta}{\rho_i\kappa}\left[\frac{T}{2}z^2 - \left(T - T_i^z\right)z\right] + \psi_0,\end{aligned} \tag{3}$$

where $C_\epsilon > 0$ denotes the specific heat capacity, $\mu > 0$ and $\lambda > -(2/3)\mu$ are the Lamé constants, T_i^z is the solid/solid phase transformation temperature when the pressure is zero, $h > 0$ is a material parameter characterizing the linear isotropic hardening associated with classical plasticity, $\delta \geq 0$ is a material parameter associated with the latent heat of the phase transformation, see Antoni [22], and ρ_i and ψ_i are the initial density and the initial Helmholtz free energy of the material, respectively, per unit mass. Note that in a first approximation, the thermoelastic parameters, C_ϵ, μ, λ, and α are not considered as function of temperature. Note also that these thermoelastic parameters are taken to be identical in the two phases.

Neglecting the viscoelastic effects and the specific entropy S is a state function, the state equations based on the above representation of Helmholtz energy (3) can be written

$$S = -\frac{\partial \psi}{\partial T}; \qquad P = -\rho \frac{\partial \psi}{\partial \ \mathrm{Tr}\ (\epsilon)};$$
$$s = \rho \frac{\partial \psi}{\partial e}; \qquad A^m = -\rho \frac{\partial \psi}{\partial m}, \tag{4}$$

in which $-P$ and s represent, respectively, the spherical and deviatoric parts of the Cauchy stress tensor, $= -PG + s$, and A^m denotes the thermodynamic forces associated with the internal variables $m = (e^{pc}, e^{pz}, \upsilon, z)$.

Using (3) and (4) and assuming that $\rho = \rho_i$, the Cauchy stress tensor reads

$$= -\frac{(3\lambda + 2\mu)}{3} \left[\mathrm{Tr}\ (\epsilon) + f(z) - 3\alpha (T - T_i) \right] G + 2\mu \left(e - e^{pz} - e^{pc} \right). \tag{5}$$

The evolution laws of the internal state variables are as follows:

(i) for the TRIP-like process

$$\dot{e}^{pz} = \dot{p} \frac{3}{2\sigma_{\mathrm{eq}}} s; \qquad \dot{z} = \kappa \dot{p}$$
$$\text{with } \dot{p} = \frac{\langle 1 - z \rangle}{\eta} \left\langle f^{pz}(T, P) \right\rangle H \left(P + \delta \left[(1 - z) T - T_i^z \right] \right) \geq 0,$$
$$f^{pz}(T, P) = \frac{T}{T_i^z} \exp\left(-\frac{\langle P \rangle}{\omega} \right), \tag{6}$$

where $P = -1/3\ \mathrm{Tr}\ (\sigma)$ is the pressure, $\omega > 0$ is a material parameter characterizing a "pressure sensitive" level, and $\langle . \rangle$ denotes the Macaulay brackets ($\langle x \rangle = x$ when $x \geq 0$ and $\langle x \rangle = 0$ when $x < 0$), η is the characteristic time of the viscous effets associated with the TRIP-like process and $H(\cdot)$ denotes the Heaviside step function ($H(x) = 1$ when $x \geq 0$ and $H(x) = 0$ when $x < 0$)

(ii) for the classical (isochoric) plasticity process

$$\dot{e}^{pc} = \dot{\upsilon} \frac{\partial f^{pc}}{\partial} = \dot{\upsilon} \frac{3}{2\sigma_{\mathrm{eq}}} s \quad \text{with } \dot{\upsilon} = \frac{\left\langle f^{pc}(, \upsilon) \right\rangle}{\xi \sigma^y} \geq 0,$$
$$f^{pc}(, \upsilon) = \sigma_{\mathrm{eq}} - \left(\sigma_y + h\upsilon \right), \tag{7}$$

where σ_{eq} is the Von Mises equivalent stress ($\sigma_{\mathrm{eq}} = (3/2\ s : s)^{1/2}$), s is the stress deviator, σ_y is the classical yield strength, and ξ is the characteristic time of the viscous effects associated with the classical plasticity.

Note that from (6)-c, in agreement with Baumann et al. [12] (who have established that applying a hydrostatic pressure decreases the temperature of the $\alpha \rightarrow \gamma$ phase transformation), the yield function is "pressure sensitive" where the temperature acts as a "driving force".

Taking account (3), (4), (6), and (7), the positiveness of the intrinsic dissipation is checked (see, e.g., [24]) that is,

$$A^{e^{pc}} : \dot{e}^{pc} + A^{\upsilon} \dot{\upsilon} + A^{e^{pz}} : \dot{e}^{pz} + A^z \dot{z} \geq 0$$
$$\forall \left(T, \mathrm{Tr}\,(\epsilon), z, \upsilon, e, e^{pz}, e^{pc} \right), \quad \forall \left(\dot{T}, \mathrm{Tr}\ (\dot{\epsilon}), \dot{e} \right), \quad \forall \nabla T \tag{8}$$

The heat equation is given by (with Fourier's law)

$$\rho_i C_\epsilon \frac{T}{T_i} \dot{T} - k\Delta T = -(3\lambda + 2\mu)\, \alpha\, T\, \mathrm{Tr}\,(\dot{\epsilon}) + s : \left(\dot{e}^{pc} + \dot{e}^{pz} \right) - h\upsilon\dot{\upsilon} + \frac{1}{\kappa} \left[P - (3\lambda + 2\mu)\, \alpha T + \delta T_i^z \right] \dot{z}, \tag{9}$$

where "Δ" denotes the Laplacian. The term on the right-hand side of (9) corresponds to the thermoelasticity, the classical plasticity and finally, the solid-solid phase transformation.

The thermomechanical model presented is thermodynamically consistent, that is, it satisfies systematically the Clausius-Duhem inequality (see, e.g., [25]) which is reduced to check only (8) since the Fourier's law is adopted.

3. Numerical Examples

Using a Return Mapping Algorithm (RMA) procedure (see, e.g., [26, 27]), the present model was implemented in the Aster finite element code (R&D/EdF).

3.1. Preliminary Remark. The example studied in this section is not representative of the complex processes occurring in wheel/rail problem. It was simply intended to show that it is possible by combining the behavioral model presented in Section 2 with a temperature field and specific mechanical boundary conditions to model the main characteristic of TSTs, namely, the fact that they occur almost only at the surface. (i) *Thermal preliminary problem*: solving the purely thermal problem with purely temperature-related boundary conditions in the stationary case. The nonuniform temperature field obtained in this way is used as a datum in the second step; (ii) *Thermomechanical problem*: solving the mechanical problem with nonuniform pressure-related boundary conditions imposed on part of the boundary and increasing linearly with time. Here, the temperature field calculated in the first step serves as a parameter.

Considering a solid occupying a square region $\Omega \in \Re^2$, measuring 100 mm aside in the x-y plane. The boundary of Ω is denoted by $\partial\Omega$ will be divided into six line segments (see also Figure 2(a)):

$$\partial\Omega = [A, B] \cup [B, C] \cup [C, D] \cup [D, E] \cup [E, F] \cup [F, A], \tag{10}$$

where $[B, C]$ is 10 mm in length. In Ω, a finite element mesh composed of approximately 20000 quadratic elements

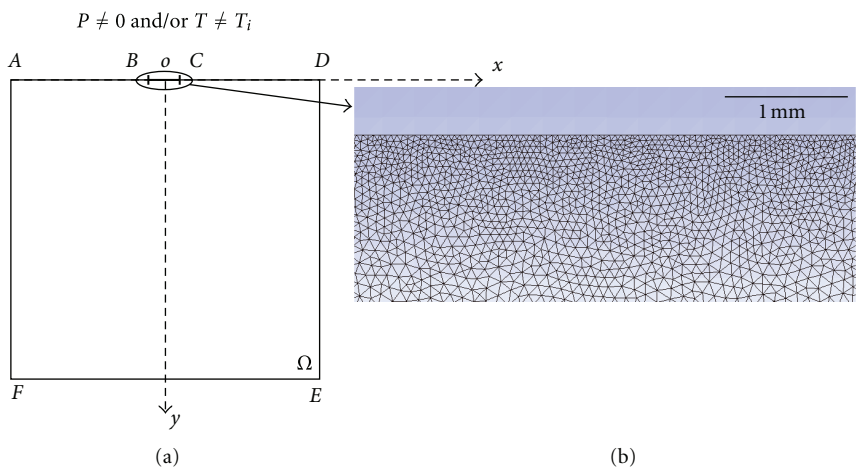

FIGURE 2: (a) Square material domain (measuring 100 mm on each side) in the x-y plane (origin: o) and boundary conditions on $[B, C]$ (where P denotes the pressure); (b) zoom of the refined mesh.

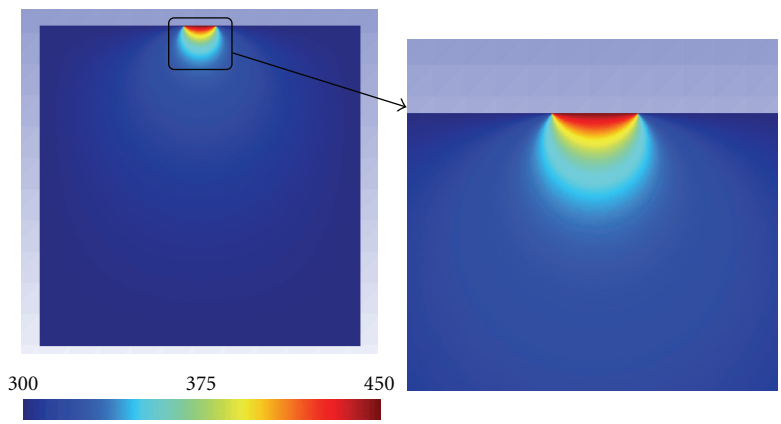

FIGURE 3: Steady temperature field (thermal problem); temperature unit: K.

is generated with a refined mesh in the vicinity of the line segment $[B, C]$ (see Figure 2(b)) where the loading is applied. This mesh is systematically used for all the numerical simulations of this section.

Thermal Preliminary Problem. The temperature field considered is plotted in Figure 3 in the steady case that is, (9) is reduced only to $\Delta T = 0$. Assuming a plane temperature field, the thermal boundary conditions in this purely thermal problem are

$$\begin{aligned} &T = T_i = 300\,K \\ &\text{on } [A, B] \cup [C, D] \cup [D, E] \cup [E, F] \cup [F, A] \\ &T = T^d = 450\,\mathrm{K} \quad \text{on } [B, C]\,. \end{aligned} \tag{11}$$

It is worth noting that (i) the room temperature is equal to the initial temperature ($T_i = 300\,\mathrm{K}$) that is, the greatest temperature increase is 150 K on $[B, C]$; (ii) the stationary thermal problem addressed in this section is quite different from the wheel/rail problem (see preliminary remark).

Thermomechanical Problem. The above temperature field presented is used as an initial datum for dealing with the thermomechanical problem. In order to satisfy the local equations of mechanical equilibrium, the stress field at the same time, $_0$, must be zero (8),

$$_0 = 0 \Longleftrightarrow \mathrm{Tr}(\epsilon_0) = 3\,\alpha\,(T_0 - T_i)\,, \tag{12}$$

where α denotes the thermal expansion coefficient which is $12 \times 10^{-6}\,\mathrm{K}^{-1}$.

The strain state is assumed to be plane and the mechanical boundary conditions are as follows:

$$\begin{aligned} &u = 0 \quad \text{on } [E, F]\,; \\ &\cdot n = 0 \quad \text{on } [A, B] \cup [C, D] \cup [D, E] \cup [F, A]\,; \\ &\cdot n = -\dot{P}^d t \left(1 - \left(\frac{x}{5}\right)^2\right)^{1/2} n \quad \text{on } [B, C] \\ &\text{with } \dot{P}^d = 100\,\mathrm{MPa} \cdot \mathrm{s}^{-1}. \end{aligned} \tag{13}$$

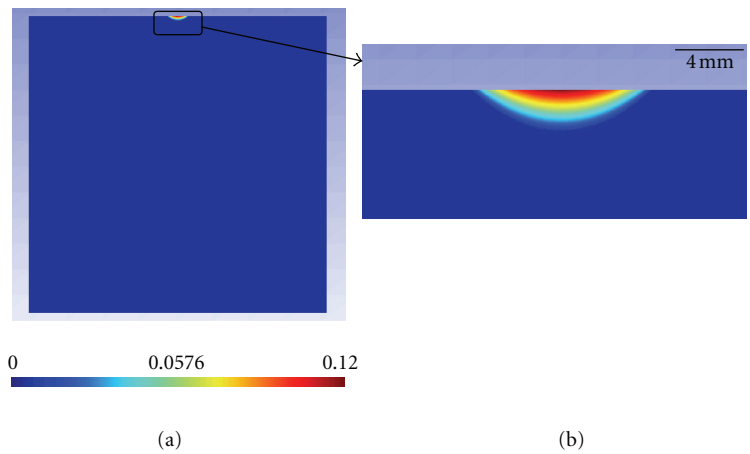

FIGURE 4: (a) z-field at time $t = 10\,\mathrm{s}$ (TRIP-like process); (b) zoom of the z-field.

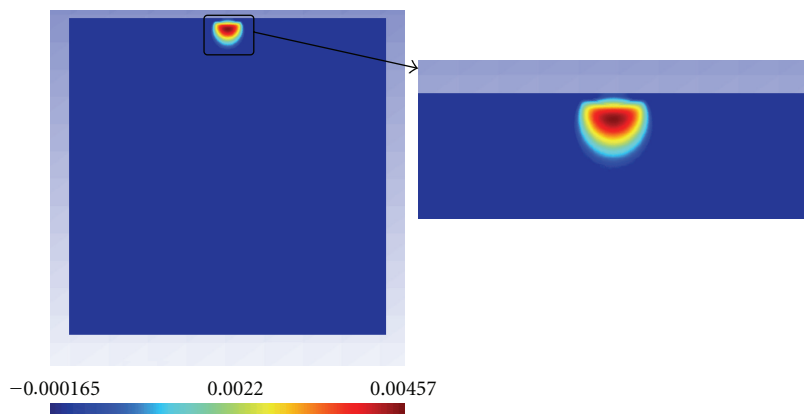

FIGURE 5: v-field at time $t = 10\,\mathrm{s}$ (classical plasticity).

Note that from (13)-c, the pressure on $[B,C]$ is maximum at $x = 0$ and equal to zero at $x = \pm 5$ mm (at points B and C). The mechanical parameters of the material are as follows:

$$\begin{gathered}\lambda = 115 \times 10^3 \text{ MPa}; \qquad \mu = 77 \times 10^3 \text{ MPa};\\ \rho_i = 78 \times 10^{-7} \text{ kg} \cdot \text{mm}^{-3}; \qquad T_i^z = 1000 \text{ K};\\ \omega = 700 \text{ MPa}; \qquad \kappa = 10^2; \qquad \eta = 10^3 \text{ s};\\ \delta = 0; \qquad \sigma_y = 400 \text{ MPa};\\ h = 2 \times 10^4 \text{ MPa}; \qquad \xi = 2.5 \times 10^2 \text{ s}.\end{gathered} \tag{14}$$

The Young's modulus E and the Poisson's ratio ν are immediately deduced from the Lamé parameters λ and μ, that is, $E = 210\,\mathrm{GPa}$ and $\nu = 0.25$. It can be seen that the characteristic times of the viscous effects associated with the TRIP-like process, η, and the classical plasticity, ξ, are small enough for the viscous effects and can be actually negligible with a characteristic loading time of this kind.

The z-field is plotted in Figure 4(a) at time $t = 10$ s, when $P(x = 0) = 1000\,\mathrm{MPa}$. It can be seen that the z-field obtained here shows the maximum phase transformation occurs near the surface and in its immediate vicinity where the mechanical loading is applied. The z-field observed is highly nonuniform: for example, along the o-y axis (see Figure 2), $z = z_{\max} \approx 12 \times 10^{-2}$ when $y = 0$ —the partial transformation at the point where the mechanical loading is applied— and $z = 6 \times 10^{-2}$ when $y \approx 9 \times 10^{-1}$ mm. The maximum transformation depth is achieved for about 17×10^{-1} mm and beyond this thickness, the nontransformed area remains. These results show that the area transformed is restricted to just a few millimeters below the surface $[B,C]$ and that the layer transformed is only partial. The v-field at time $t = 10\,\mathrm{s}$ is plotted in Figure 5. It can be seen that v is zero on $[B,C]$, where the mechanical loading is applied, and reaches a maximum value around 45×10^{-4} in Ω. Note also that that there exists a small area, just below the surface, where both v and z (see Figure 4) are nonzero; the TRIP-like processes and classical plasticity are closely correlated.

Although the example studied does not take into account the nonlinear contact and friction between wheel and rail, the results obtained tend to show that the model proposed (see Section 2) may predict the experimental data, especially those relating to TSTs on railway tracks. In this matter, the specific material parameters of the model will have to be precisely identified in experimental works.

4. Conclusion

In this paper, a thermodynamically consistent thermomechanical model was presented in order to describe initiation and development of the Tribological Surface Transformations (TSTs). Based on the conjecture that TSTs have a thermomechanical origin that is, TSTs are due to combined thermomechanical loads, the model proposed presents the main advantage to have a small number of specific material parameter, T_i^z, ω, δ, κ, and η, except the classical thermoelastic parameters which are known. Some numerical examples have been proposed to assess the ability of the model to predict these TSTs. The results obtained show that the solid-solid phase transformations can be achieved in the immediate vicinity of the surface where the mechanical loading is applied. Therefore, the thermomechanical model developed will be tested on the wheel/rail problem in the future work.

References

[1] C. Colombié, *Usure induite sous petits débattements-Identification des phénomènes [Thèse de doctorat]*, INSA Lyon, France, 1986.

[2] P. Blanchard, *Usure induite en petits débattements: transformation tribologique superficielle d'alliages de titane [Thèse de doctorat]*, INSA Lyon, France, 1991.

[3] E. Sauger, *Contribution à l'étude de la transformation tribologique superficielle en fretting [Thèse de doctorat]*, INSA Lyon, France, 1997.

[4] A. C. Sekkal, *Etude des transformations tribologiques de surfaces ou TTS induites par impacts à énergie controlée [thèse de doctorat]*, INSA Lyon, France, 2000.

[5] W. Österle, H. Rooch, A. Pyzalla, and L. Wang, "Investigation of white etching layers on rails by optical microscopy, electron microscopy, X-ray and synchroton X-ray diffraction," *Materials Science and Engineering A*, vol. 303, no. 1-2, pp. 150–157, 2001.

[6] W. Lojkowski, M. Djahanbakhsh, G. Bürkle, S. Gierlotka, W. Zielinski, and H. J. Fecht, "Nanostructure formation on the surface of railway tracks," *Materials Science and Engineering A*, vol. 303, no. 1-2, pp. 197–208, 2001.

[7] A. Pyzalla, L. Wang, E. Wild, and T. Wroblewski, "Changes in microstructure, texture and residual stresses on the surface of a rail resulting from friction and wear," *Wear*, vol. 251, no. 2, pp. 901–907, 2001.

[8] E. Wild, L. Wang, B. Hasse, T. Wroblewski, G. Goerigk, and A. Pyzalla, "Microstructure alterations at the surface of a heavily corrugated rail with strong ripple formation," *Wear*, vol. 254, no. 9, pp. 876–883, 2003.

[9] M. Hiensch, J. C. O. Nielsen, and E. Verheijen, "Rail corrugation in the Netherlands—measurements and simulations," *Wear*, vol. 253, no. 1-2, pp. 140–149, 2002.

[10] J. F. Archard and R. A. Rowntree, "The temperature of rubbing bodies; the distribution of temperatures," *Wear*, vol. 128, pp. 1–17, 1988.

[11] J. Ahlström and B. Karlsson, "Microstructural evaluation and interpretation of the mechanically and thermally affected zone under railway wheel flats," *Wear*, vol. 232, no. 1, pp. 1–14, 1999.

[12] G. Baumann, H. J. Fecht, and S. Liebelt, "Formation of white-etching layers on rail treads," *Wear*, vol. 191, no. 1-2, pp. 133–140, 1996.

[13] Y. Jirásková, J. Svoboda, O. Schneeweiss, W. Daves, and F. D. Fischer, "Microscopic investigation of surface layers on rails," *Applied Surface Science*, vol. 239, no. 2, pp. 132–141, 2005.

[14] G. W. Greenwood and R. H. Johnson, "The deformation of metals under small stresses during phase transformations," in *Proceedings of the Royal Society of London*, vol. 293 of *Mathematical and Physique Sciences*, pp. 403–422, 1965.

[15] J. B. Leblond, J. Devaux, and J. C. Devaux, "Mathematical modelling of transformation plasticity in steels I: case of ideal-plastic phases," *International Journal of Plasticity*, vol. 5, no. 6, pp. 551–572, 1989.

[16] J. B. Leblond, "Mathematical modelling of transformation plasticity in steels II: coupling with strain hardening phenomena," *International Journal of Plasticity*, vol. 5, no. 6, pp. 573–591, 1989.

[17] J.-C. Videau, G. Cailletaud, and A. Pineau, "Modélisation des effets mécaniques des transformations de phases pour le calcul de structures," *Journal de Physique IV*, vol. 4, no. 3, pp. 227–232, 1994.

[18] J.-C. Videau, G. Cailletaud, and A. Pineau, "Experimental study of the transformation-induced plasticity in a Cr-Ni-Mo-Al-Ti steel," *Journal De Physique. IV*, vol. 6, no. 1, pp. 465–474, 1996.

[19] F. D. Fischer, G. Reisner, E. Werner, K. Tanaka, G. Cailletaud, and T. Antretter, "New view on transformation induced plasticity (TRIP)," *International Journal of Plasticity*, vol. 16, no. 7, pp. 723–748, 2000.

[20] L. Taleb and F. Sidoroff, "A micromechanical modeling of the Greenwood-Johnson mechanism in transformation induced plasticity," *International Journal of Plasticity*, vol. 19, no. 10, pp. 1821–1842, 2003.

[21] L. Taleb and S. Petit, "New investigations on transformation induced plasticity and its interaction with classical plasticity," *International Journal of Plasticity*, vol. 22, no. 1, pp. 110–130, 2006.

[22] G. Antoni, T. Désoyer, and F. Lebon, "Tribological transformations of surface: a thermo-mechanical modelling," in *Proceedings of the 10th International Conference on Computational Structures Technology*, p. 14, 2010, (CD-ROM).

[23] G. Antoni, *Transformation tribologique de surface: une approche thermo-mécanique [Thèse de doctorat]*, Université de Provence, France, 2010.

[24] J. Garrigues, *Fondements de la Mécanique des milieux continus*, Hermés Science Publications, France, 2007.

[25] J. Lemaitre and J. L. Chaboche, *Mécanique des Matériaux Solides*, Dunod, France, 1996.

[26] Q. S. Nguyen, "On the elastic-plastic initial-boundary value problem and its numerical integration," *International Journal for Numerical Methods in Engineering*, vol. 11, no. 5, pp. 817–832, 1977.

[27] J. C. Simo and R. L. Taylor, "Consistent tangent operators for rate-independent elastoplasticity," *Computer Methods in Applied Mechanics and Engineering*, vol. 48, no. 1, pp. 101–118, 1985.